NASA TECHNICAL NOTE

NASA TN D-5222

NASA TN D-5222

ON THE PHENOMENON OF THERMOELASTIC INSTABILITY (THERMAL FLUTTER) OF BOOMS WITH OPEN CROSS SECTION

by Richard M. Beam

Ames Research Center
Moffett Field, Calif.

NATIONAL AERONAUTICS AND SPACE ADMINISTRATION • WASHINGTON, D. C. • JUNE 1969

ON THE PHENOMENON OF THERMOELASTIC INSTABILITY (THERMAL FLUTTER) OF BOOMS WITH OPEN CROSS SECTION

By Richard M. Beam

Ames Research Center
Moffett Field, Calif.

NATIONAL AERONAUTICS AND SPACE ADMINISTRATION

For sale by the Clearinghouse for Federal Scientific and Technical Information
Springfield, Virginia 22151 – CFSTI price $3.00

ON THE PHENOMENON OF THERMOELASTIC INSTABILITY (THERMAL FLUTTER) OF BOOMS WITH OPEN CROSS SECTION

By Richard M. Beam

Ames Research Center

SUMMARY

Satellites with long extendible appendages (booms) of open cross section have experienced unstable oscillations. Telemetered data on the frequency of oscillation and satellite exposure to solar radiation suggest that the instability results from a thermoelastic flutter of the booms. Laboratory experiments performed to demonstrate the phenomenon of thermoelastic flutter are described.

The problem of torsional instability is chosen for theoretical treatment and comparison with quantitative experimental results. The theoretical and experimental models show that (1) one-degree-of-freedom torsional thermoelastic flutter is possible and predictable, (2) thermoelastic coupling can stabilize as well as destabilize a system, and (3) small amplitude linear theory can predict thermoelastic instability.

INTRODUCTION

Various satellite applications require long extendible appendages (booms) as a part of the design configuration. One design of a deployable boom is shown schematically in figure 1. The diameters of these booms are generally about 1/2 in. and the length varies from a few feet to several hundred feet. This type of boom has been used successfully in many satellites for antennas, gravity gradient stability augmentation, and isolation of equipment and experiments from the satellite.

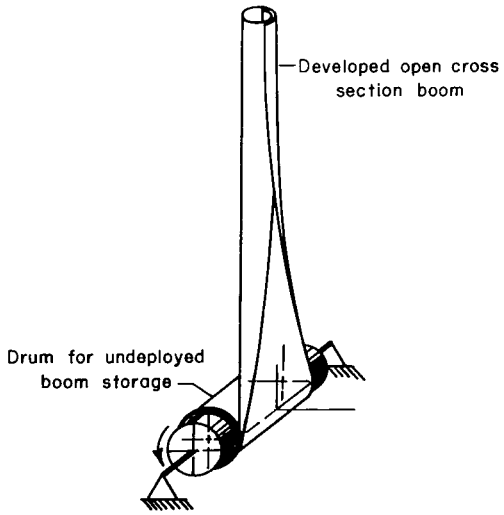

Figure 1.- Deployable boom.

Telemetered data from the Orbiting Geophysical Observatory (OGO) satellite indicated that at various times the satellite experienced oscillations of increasing amplitude. The frequency of the unstable oscillations was the same as the natural frequency of the booms attached to the satellite. It was further noted that the oscillations began as the satellite moved from the earth's shadow into

the sunlight and subsequently decayed when the satellite re-entered the earth's shadow. The frequency of the oscillations and their occurrence only when the satellite was exposed to sunlight led to conjecture that the instability was a result of the coupling of the thermal radiation from the sun and the elastic deformations of the booms.

In May 1968, the observed phenomenon was brought to the attention of the author. Because of the lack of any physical evidence of the phenomenon (other than the limited flight data noted above), an experimental laboratory program was initiated. The primary goal of this program was the laboratory demonstration of thermoelastic instability. Since booms of open cross section were being used on the flight where the instability was observed, a similar material was chosen for the laboratory experiments.

The first successful demonstration (June 4, 1968) was performed with a 3-ft-long boom that was fixed at one end and had an attached tip mass at the other (fig. 2). The boom material was beryllium copper with a diameter of 1/2 in. and a wall thickness of 0.002 in. The boom was painted black to increase thermal absorptivity, and the thermal source was provided by photoflood lamps. The boom had an overlapping cross section (section A-A, fig. 2). The system was observed to be stable for small amplitude motions but unstable (oscillatory increasing amplitude) for larger amplitudes with eventual limit cycle oscillation in a coupled torsional bending mode. The limit cycle oscillation amplitudes consisted of tip mass deflections of several inches (normal to the plane of the light) and tip mass rotations of ±90°.

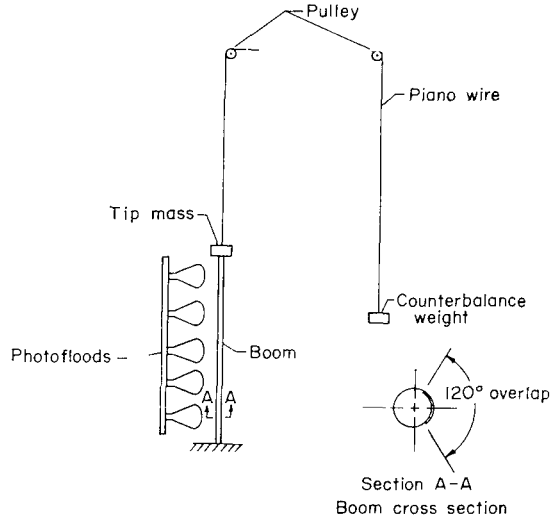

Figure 2.- Test arrangement for initial demonstration of thermoelastic instability.

Additional demonstrations of thermal flutter were made using an unpainted boom of the same material but 19 ft long. The boom was hung from its fixed end, and demonstrations were made with and without small tip masses (1/2-in. steel cylinders approximately 3 in. long, mounted coaxially with the boom). In each case a coupled torsional bending mode of flutter was obtained.

The observed behavior of the boom during these experiments suggested the possibility of a one-degree-of-freedom torsional flutter. To check this, a large (8-in.-diameter, 1/4-in.-thick) disc was attached to the end of the 19-ft-long boom. The resulting flutter was almost pure torsion with rotational limit cycle amplitude of the tip disc reaching ±3 revolutions while the tip deflected only 3 in. In addition, tests were conducted with the tip mass fully restrained from lateral deflection. These demonstrations were recorded in a 16 mm color, sound film which is available on loan from the author (R. M. Beam, mail stop 242-1, Ames Research Center, Moffett Field, Calif., 94035).

Theoretical development was initiated concurrently with the experimental program. The goal of this program was to develop an understanding of the basic phenomenon and to provide an analytical model that would aid in predicting thermal flutter. To simplify the mechanics of the problem, the initial analytical approach was based on a linearized one-degree-of-freedom (torsional) model suggested by the above experiments. The purpose of this report is to describe the results of the theoretical program and to compare them with the measured data obtained from the experiments.

Several papers have become available to the author during the preparation of this report (refs. 1-4). Each presents an analytical treatment of a thermoelastic problem. Augusti (ref. 1) considers the bending of a cantilever strut idealized as either a one- or two-degree-of-freedom system subjected to radiant heat parallel to the axis of the strut. Yu (ref. 2) considers a generalization of the same problem. He treats the beam as a continuum, uses a modal-type solution, and allows different angles of inclination of the beam with the heat source. The criteria for flutter reached by Augusti and Yu are completely contradictory. After a cursory examination of both papers, this author is inclined to agree with the criteria of Augusti. The discrepancy with Yu apparently comes from his treatment of "time lag."

Koval, Mueller, and Paroczai (ref. 3) present a theory for an initially straight boom of open cross section simulating the OGO-IV spacecraft. Both twisting and bending of the boom are allowed. Results are given in the form of numerical solutions to the derived equations.

Donohue and Frisch (ref. 4) discuss the results (without presenting the formulation) of a program similar to that of Koval et al. Again the results are presented as numerical solutions to the derived equations.

Additional analysis of coupled modes and large amplitudes will undoubtedly lead to interesting results. The initial experiments described above indicate that systems which are stable for small amplitudes can be unstable for large amplitudes. However, the small amplitude analysis may prove adequate for the determination of the stability of systems subjected to small perturbations about an equilibrium configuration.

The author wishes to thank Ralph Abbott of Spar Aerospace Products Limited, who provided the boom material for the experimental program.

NOMENCLATURE

B steady-state radiation input to boom

C_1 warping rigidity of boom

c_E coefficient of structural damping in pendulum

E modulus of elasticity

h wall thickness of boom used for torsional spring

I_m polar mass moment of inertia of tip mass of torsional pendulum about center of rotation

K_E elastic spring constant of torsional pendulum

K_1 constant defined by equation (16)

K_3 constant defined by equation (18)

l length of boom used for torsional spring

M_t torsional moment in boom

R perturbation radiation input to boom

r radius of boom used for torsional spring

S parameter in characteristic equation

s_n root of characteristic equation

T change in boom temperature during perturbation about equilibrium position

t time

w total length of "rolled out" cross section of tube ($2\pi r$ for non-overlapped tube)

x coordinate along boom (origin at fixed end)

α coefficient of expansion for boom material

β thermal constant (eq. (8))

ζ damping coefficient (eq. (20))

Θ total angular deformation of pendulum tip mass

Θ_E angular deformation of pendulum tip mass due to inertial loading

Θ_T angular deformation of pendulum mass due to thermal loading

θ angular displacement of boom cross section

λ function defined by equation (9)

ϕ angular coordinate of point on surface of boom

Ψ angle between thermal source and equilibrium axis of symmetry of boom (fig. 3)

ω_o natural frequency of torsional pendulum (eq. (19))

$(\bar{\ })$ dummy variable of integration

$(\dot{\ })$ differentiation with respect to time

$(')$ differentiation with respect to x

ANALYSIS

Basic Model

The model discussed in this report was chosen because it leads to a simple mathematical analysis and yet demonstrates one of the basic mechanisms of thermoelastic coupling. In addition, it provides a simple physical analogy from which quantitative experimental data can be obtained for comparison with the theoretical assumptions.

Consider the dynamics of the torsional pendulum illustrated in figures 3 and 4. The elastic spring of the pendulum is a split non-overlapping boom. The upper end of the boom is rigidly fixed and warping of the cross section of the boom is prevented. A mass is attached to the lower end of the boom, which is free to warp. The tip mass is restrained from lateral displacement by a low friction bearing. If the inertia of the tip mass is large compared with that of the tube, the system can be analyzed as a simple one-degree-of-freedom mechanism.

Let Θ denote the total angular rotation of the tip mass and I_m the mass moment of inertia of the tip mass, then the torque acting on the tip of the boom is $-I_m\ddot{\Theta}$. This torque is partially balanced by the torque of the

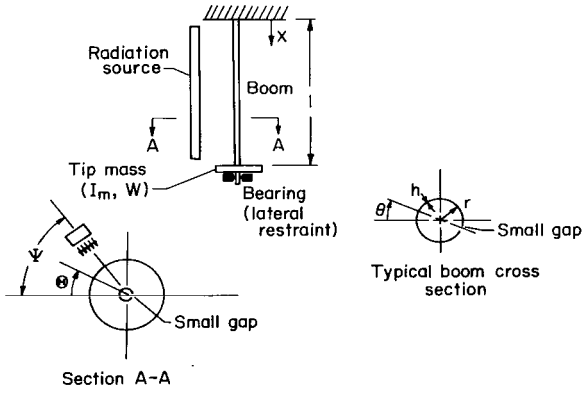

Figure 3.- Analytical model and physical model used in torsional pendulum investigation.

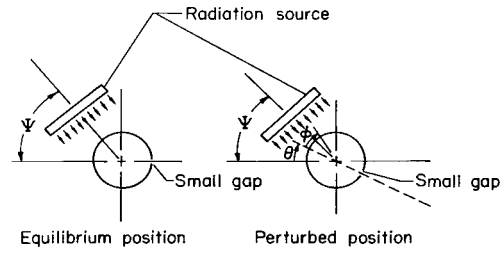

Figure 4.- Geometry for thermal deformation analysis.

elastic restoring forces, $K_E\Theta_E$, where Θ_E is the elastic deformation of the boom tip and K_E the elastic spring constant of the boom. In addition, there is a damping torque, $c_E\dot{\Theta}_E$ (assumed proportional to the elastic deformation); therefore

$$I_m\ddot{\Theta} + c_E\dot{\Theta}_E + K_E\Theta_E = 0 \tag{1}$$

The total deformation Θ differs from the elastic deformation, Θ_E, by the amount of thermal deformation, Θ_T; therefore,

$$\Theta = \Theta_E + \Theta_T \tag{2}$$

Elastic Deformation

If the angular rotation of the boom at station x at time t is denoted by $\theta(x, t)$, then the torque in the boom, M_t (assumed constant along the length), is (ref. 5)

$$M_t = C\frac{\partial\theta_E}{\partial x} - C_1\frac{\partial^3\theta_E}{\partial x^3}$$

where C is the torsional rigidity and C_1 the warping rigidity.

When the boom wall thickness h is much less than the boom diameter, $2r(h << 2r)$, and the boom length l is not too great, then $Cl^2 << C_1$ and it can be shown (ref. 6) that a good approximation to M_t is

$$M_t = -C_1\frac{\partial^3\theta_E}{\partial x^3} \tag{3}$$

where C_1, the warping rigidity,[1] is (ref. 5)

$$C_1 = \frac{1}{12}w^3r^2hE \tag{4}$$

In this model the upper end of the boom ($x = 0$) is fixed and restrained from warping while the lower end is free to warp; therefore, the boundary conditions for equation (3) are

$$\theta_E(0) = 0, \qquad \theta_E'(0) = 0, \qquad \theta_E''(l) = 0 \tag{5}$$

The solution for equation (3) with boundary conditions (5) is

$$\theta_E = \frac{M_t l}{C_1}\left(\frac{x^2}{2} - \frac{x^3}{6l}\right) \tag{6}$$

---

[1]The boom is assumed to be constrained to rotate about the geometric center of the circular cross section. For rotations about the shear center the warping rigidity would be reduced. The pendulum is assumed to be sufficiently short that the effect of torsional rigidity is negligible when compared to the effect of warping rigidity.

The spring constant, K_E, of the torsional pendulum is

$$K_E = \frac{M_t}{\theta_E(l)}$$

or

$$K_E = \frac{3C_1}{l^3} \tag{7}$$

Thermal Deformation

The amplitudes and frequencies of the model will be restricted to those for which the temperature perturbation due to change of radiation input (with time) is large compared to the temperature perturbation due to change in conduction around the cross section. The analysis will be based on small perturbations about an equilibrium configuration. The system is assumed to have reached an equilibrium temperature distribution (the absorption from thermal radiation balanced by the output due to emission from the entire surface) before it is disturbed.

If the source temperature remains constant and the tube temperature changes are not large during the perturbations, then the boom temperature, T, can be expressed as (ref. 7)

$$\frac{\partial T}{\partial t} + \beta T = R(x,\phi,t) \tag{8}$$

where β and R depend on the source of radiation and the properties of the boom.[2] It is assumed that the boom is thin walled and the temperature through the thickness does not vary.

If the radiation source is a uniform parallel field as shown in figure 4, the normal radiation input, Q, which produces the equilibrium temperature distribution in the tube is $(-\pi \leq \phi \leq +\pi)$

$$Q(\phi) = \lambda B \cos(\phi - \Psi)$$

where λ is unity for values of ϕ corresponding to the portion of boom surface exposed to radiation and is zero otherwise. For $0 \leq \Psi \leq \pi$, λ is defined by the conditions

---

[2]Equation (8) is obtained from the equation of radiation input (proportional to the difference of the fourth powers of the body and source) and change in internal energy of the body. The linearization is possible if the difference between body and source temperature experiences only small changes. The constants β and R depend on the radiation boundary conductance, specific heat and density of the material, and the thickness of the boom. Additionally, R depends on the temperature of the source.

$$0 \le \Psi \le \frac{\pi}{2} \quad \begin{cases} \lambda = 1 & \text{if } -\frac{\pi}{2} \le \phi - \Psi \le \frac{\pi}{2} \\ = 0 & \text{otherwise} \end{cases} \tag{9}$$

$$\frac{\pi}{2} \le \Psi \le \pi \quad \begin{cases} \lambda = 1 & \text{if } \begin{cases} \Psi - \frac{\pi}{2} \le \phi \le \pi \\ -\pi \le \phi \le -\frac{3}{2}\pi + \Psi \end{cases} \\ = 0 & \text{otherwise} \end{cases}$$

As the cross section of the boom rotates through an angle θ, the change in radiation is

$$R(x,\phi,t) = \lambda B \cos(\phi - \Psi + \theta) - \lambda B \cos(\phi - \Psi)$$

For small rotation (θ) of the cross section R can be approximated by

$$R(x,\phi,t) = -\lambda B \sin(\phi - \Psi)\theta(x,t) \tag{10}$$

If the perturbation temperature, T, is assumed to be zero at time zero [$T(x,\phi,0) = 0$], then from equations (8) and (10)

$$T(x,\phi,t) = -e^{-\beta t} \int_0^t \lambda B \sin(\phi - \Psi)\theta(x,\bar{t})e^{\beta \bar{t}}\, d\bar{t} \tag{11}$$

Note that $T(x,\phi,t)$ describes the perturbation temperature over the surface of the boom.

The thermal deformations will, in general, be quite small compared with the elastic deformations. Therefore, the geometric distortion can be assumed to be proportional to the elastic deformation shape (eq. (6)).

$$\theta(x,t) \approx \Theta(t)\, \frac{3}{l^2} \left(\frac{x^2}{2} - \frac{1}{l}\frac{x^3}{6}\right) \tag{12}$$

The proportionality constant was chosen so that $\theta(l,t) = \Theta(t)$.

The thermal deformation due to the perturbation temperature T is[3]

$$\frac{\partial^3 \theta_T}{\partial x^3} = \frac{12\alpha r}{w^3} \int_{-\pi}^{\pi} \int_{-\pi}^{\phi} \frac{\partial T}{\partial x}\, d\bar{\phi}\, d\phi \tag{13}$$

[3]This relation can be obtained from reference 5 if the stress strain relation $\sigma = E\varepsilon$ is replaced by $\sigma = E(\varepsilon - \alpha T)$, which includes the effect of thermal "strains." After evaluation of the shear stress, the torque is obtained by integration over the cross-sectional area of the boom, and equation (13) is obtained.

Substitution of the temperature distribution T from equation (11), with the approximation for θ (eq. (12)) into equation (13), leads to

$$\frac{\partial^3 \theta_T}{\partial x^3} = -\frac{12\alpha r}{w^3} e^{-\beta t} \int_0^t \Theta(\bar{t}) e^{+\beta \bar{t}}\, d\bar{t} \left[\frac{3}{l^2}\left(x - \frac{1}{2}\frac{x^2}{l}\right)\right] \int_{-\pi}^{\pi}\int_{-\pi}^{\phi} \lambda B \sin(\bar{\phi} - \Psi) d\bar{\phi}\, d\phi \tag{14}$$

After integration of equation (14) three times with respect to x and application of the boundary conditions at the upper end of the boom

$$\theta_T(0) = \frac{\partial \theta_T(0)}{\partial x} = \frac{\partial^2 \theta_T(0)}{\partial x^2} = 0$$

and at the lower end of the boom

$$\theta_T(l) = \Theta_T$$

the result is

$$\Theta_T = \frac{6\alpha r l^2}{5w^3} K_1(\Psi) B e^{-\beta t} \int_0^t e^{\beta \bar{t}}\, \Theta(\bar{t}) d\bar{t} \tag{15}$$

where

$$K_1(\Psi) = -\int_{-\pi}^{\pi}\int_{-\pi}^{\phi} \lambda \sin(\bar{\phi} - \Psi) d\bar{\phi}\, d\phi = \begin{cases} 2 & 0 \le \Psi \le \frac{\pi}{2} \\ 2(1 + \pi \cos \Psi) & \frac{\pi}{2} \le \Psi \le \pi \end{cases} \tag{16}$$

$K_1(\Psi)$ is plotted in figure 6.

System Damping and Stability

The equations of motion of the torsional pendulum perturbed about an equilibrium position are given by equations (1), (2), and (15), or

$$\left.\begin{aligned} \ddot{\Theta} + 2\zeta\omega_o \dot{\Theta}_E + \omega_o^2 \Theta_E &= 0 \\ \Theta &= \Theta_E + \Theta_T \\ \dot{\Theta}_T + \beta \Theta_T &= K_3(\Psi)\Theta \end{aligned}\right\} \tag{17}$$

where equation (15) has been differentiated with respect to time, and

$$K_3(\Psi) = \frac{6\alpha r \ell^2}{5w^3} K_1(\Psi)B \tag{18}$$

$$\omega_o = \sqrt{K_E/I_m} \tag{19}$$

$$\zeta = \frac{c_E}{2\omega_o I_m} \tag{20}$$

The characteristic equation for the system of equations (17) is

$$(s + \beta)(s^2 + 2\zeta\omega_o s + \omega_o^2) - K_3(2\zeta\omega_o s + \omega_o^2) = 0 \tag{21}$$

Therefore, the pendulum displacement θ is

$$\theta = \sum_{n=1}^{3} A_n e^{s_n t}$$

where s_n (n = 1, 2, 3) denotes the roots of the characteristic equation (21) and A_n denotes constants determined by the initial conditions.

The roots of equation (21) are either (a) three real roots or (b) one real root and a complex pair of roots. The system stability depends only on the sign of the real part of the roots (a positive real part indicating instability). In general, for the torsional pendulum the roots will be of type (b). The type of instability observed in the tests (to be discussed later) has a negative real root, and the real part of the complex pair of roots is positive, thus the motion is oscillatory divergent or "flutter." A positive real root (negative real part of complex pair) corresponds to the divergent nonoscillatory or thermal buckling mode of instability.

From Routh's stability criterion (ref. 8) it can be shown that the real part of all roots of equation (21) is negative (stable system), provided

$$\left.\begin{aligned} &2\zeta\omega_o + \beta > 0 \\ &K_3 - \frac{2\zeta\omega_o^2 + 4\zeta^2\omega_o\beta + 2\beta^2\zeta}{4\zeta^2\omega_o + 2\zeta\beta - \omega_o} > 0 \\ &\beta - K_3 > 0 \end{aligned}\right\} \tag{22}$$

No structural damping.- Consider first the case of zero structural damping ($c_E = 0$). The characteristic equation (21) reduces to

$$(s + \beta)(s^2 + \omega_o^2) - K_3\omega_o^2 = 0 \tag{23}$$

and the stability criteria, equation (22), reduce to

$$\beta > 0$$

$$K_3 > 0$$

$$\beta > K_3$$

or since β is a positive number, simply

$$0 < K_3 < \beta$$

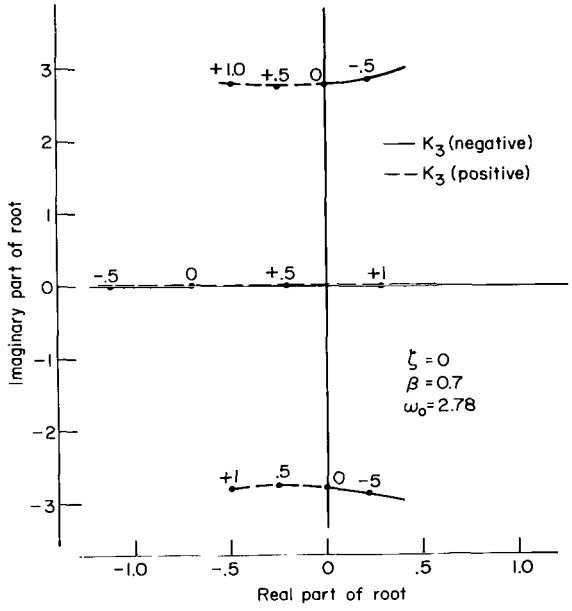

Figure 5.- Root locus for torsional pendulum characteristic equation (no structural damping).

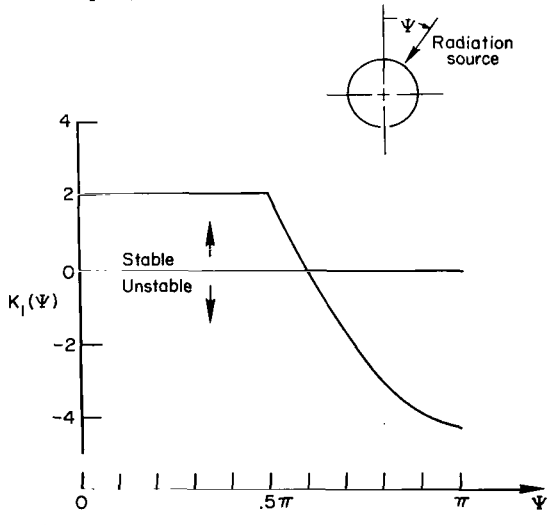

Figure 6.- Function $K_1(\Psi)$ evaluated from equation (16).

The locus of the roots of equation (23) for positive and negative values of K_3 is shown in figure 5. The following conclusions can be drawn from figure 5 and the stability criteria:

(a) For K_3 negative, the pendulum will be unstable and have an oscillatory divergent motion (i.e., flutter).

(b) For K_3 positive, the pendulum will be stable provided $K_3 < \beta$. If $K_3 > \beta$ the motion of the pendulum will be divergent (nonoscillatory) or the pendulum will experience thermal buckling.

Since β is positive (source hotter than pendulum), the sign of K_3 (eq. (18)) has the same sign as K_1. The value of K_1 is shown in figure 6. For the pendulum with no structural damping, we may conclude, therefore, that the position of the source determines the stability of the pendulum in the flutter mode. For angles Ψ less than 108°, the pendulum will not flutter, and for angles greater than 108° the pendulum will flutter. If the value of K_3 is positive and greater than β, the pendulum will experience thermal buckling.

Structural damping.- For small values of structural damping the conclusions of the previous section are little changed. The locus of the roots of the characteristic equation is shown in

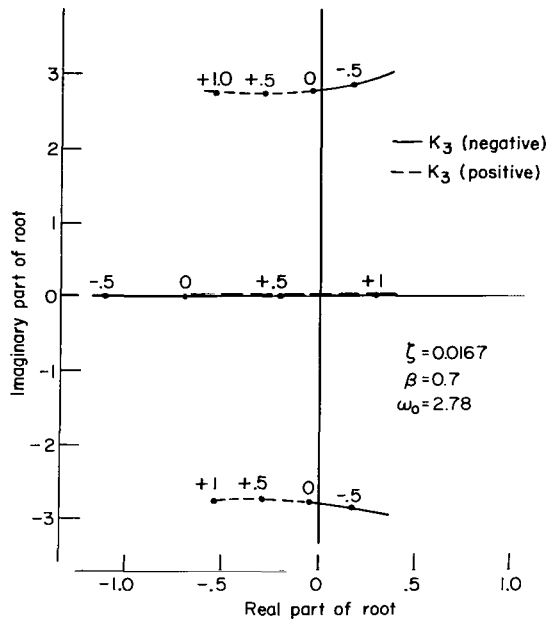

Figure 7.- Root locus of torsional pendulum characteristic equation (with structural damping).

figure 7. Since β, ζ, and ω_o are positive, the stability criteria (eq. (22)) reduce to

$$\frac{2\zeta\omega_o^2 + 4\zeta^2\omega_o\beta + 2\beta^2\zeta}{4\zeta^2\omega_o + 2\zeta\beta - \omega_o} < K_3 < \beta$$

The primary difference caused by the structural damping is that larger absolute values of K_3 are required to produce flutter in the pendulum.

Note that for two thermal sources, one of each located at $\Psi = 0$ and $\Psi = \pi$, the total K_1 value is negative $[2 - 2(\pi - 1) \approx -2.28]$. Thus this heating configuration leads to an unstable system for low values of structural damping.[4] This conclusion has been demonstrated experimentally.

EXPERIMENTS

Arrangement

The experiments to obtain quantitative data were conducted on a pendulum with the following properties:

$r = 0.125$ in. $\quad I_m = 0.00258$ lb in. sec^2

$l = 13.5$ in. $\quad E = 17\times10^6$ lb in.$^{-2}$

$h = 0.00144$ in. $\quad \alpha = 17.8\times10^{-6}$ °C^{-1}

The torsional spring boom was beryllium copper. The exterior surface of the tube was painted flat black to increase the thermal absorptivity coefficient. The heat source was a tubular, quartz, tungsten-filament, infrared lamp. A parabolic ceramic reflector was used to direct most of the lamp's thermal output in parallel rays over the surface of the tube. The distance between the lamp filament and tube center line was four inches.

[4]This observation may have particular significance in the application of the booms designed with perforations. The perforations are chosen so that the surfaces away from and toward the sun have the same radiation input and thus prohibit bending of the booms. Uniform radiation on both sides of the boom, however, does not necessarily ensure that the thermal "damping" will be zero.

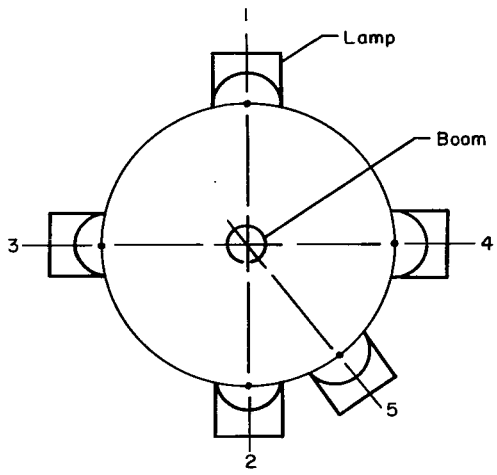

Figure 8.- Lamp arrangement for bell jar experiments.

The tests were conducted in a bell jar with absolute pressure less than 0.5 mm Hg. The vacuum was used to remove the effects of laboratory and convective currents from the measurements. To expedite the data acquisition, lamps were placed at several locations around the tube (fig. 8).

Test Procedure

Lamps 1, 2, and 5 could be operated independently but 3 and 4 were operated in unison. After the bell jar was evacuated to an absolute pressure of less than 0.5 mm Hg, the damping measurements were conducted as indicated below:

(a) (Divergent oscillations, unstable motion, $\Psi = 180°$) Lamp number 2 was turned on and temperature distribution allowed to reach steady state (1 or 2 min). Although the system is, in general, unstable with only lamp number 2 on, this procedure could be accomplished by very precise alinement of the tube so that the input disturbance from lamp turn-on was minimized. Next, lamp number 5 was briefly turned on (approximately 1 sec) to provide a system disturbance. The response of the system (growth in amplitude) was recorded on high-speed motion picture film (100 frames/sec) for later analysis.

(b) (Convergent oscillations, stable motion, $\Psi = 0°$) After large amplitude motion ($\approx \pm 90°$) was obtained as in step (a), lamp number 2 was turned off and lamp number 1 turned on. The subsequent decay of pendulum amplitude was recorded on film.

(c) (Structural damping coefficient, no lamp) The amplitude was increased to the desired level, as in step (a). Then all lamps were turned off, and the decay due to structural damping was recorded.

(d) (Convergent oscillations, stable motion, two lamps, $\Psi = \pm 90°$) The measurement of damping for lamp positions other than $\Psi = 0°$ and $\Psi = 180°$ requires that the lamps be used in pairs to maintain the equilibrium symmetry of the tube. Thus lamps 3 and 4 were operated in unison, and step (c) was repeated to obtain data for $\Psi = 90°$.

Results of Experiments

The films were read to determine the positive and negative amplitudes at successive peaks. Typical amplitude decay curves are shown on semilog plots

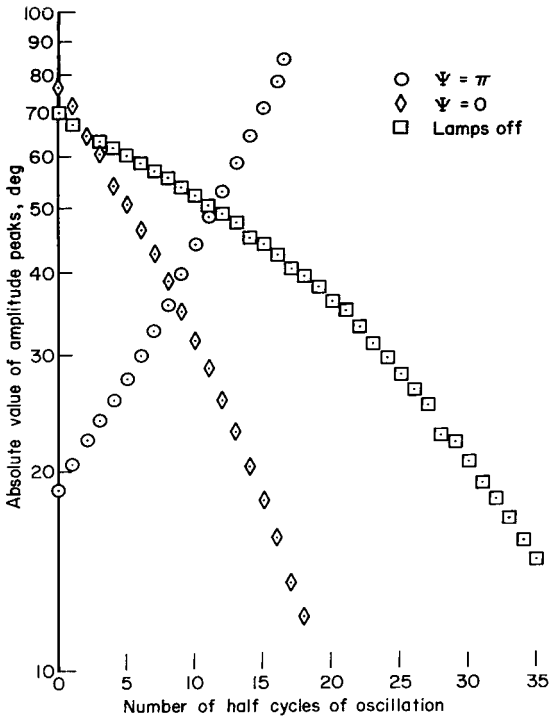

Figure 9.- Absolute value of amplitude peaks vs. number of half cycles of oscillation of torsional pendulum for various lamp positions.

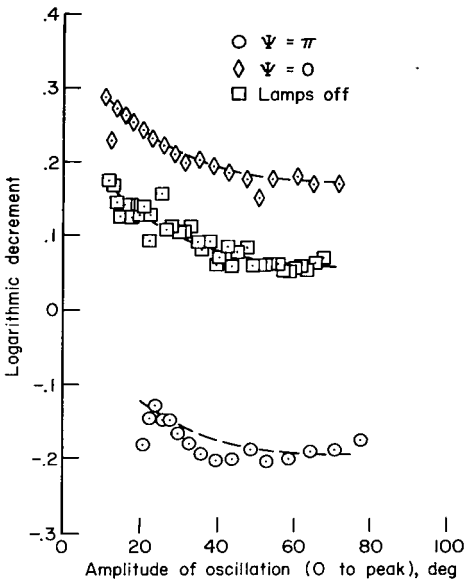

Figure 10.- Logarithmic decrement vs. amplitude of oscillation of torsional pendulum for various lamp positions.

in figure 9. A purely exponential decay would, of course, lie along a straight line. The lack of a good straight line fit for the "lamps off" case indicates that the structural damping is slightly nonlinear. The logarithmic decrement was plotted as a function of amplitude to obtain the change in damping due to "lamps on." That is, the logarithmic decrement was computed for each cycle on the basis of the decay for that cycle. The results of these computations are shown in figure 10. Note that over a wide range of amplitudes the difference between the logarithmic decrement with "lamps on" and damping with "lamps off" appears more or less constant. This indicates that the nonlinearity in the system decay (nonexponential) could be due to nonlinear system structural damping alone. Resolution (to approximately 1° amplitude) of the data film prohibited obtaining reliable decay data for the amplitude range $-12° < \theta < +12°$.

Determination of B and β

Comparison of theoretical and experimental results requires a knowledge of the parameters B and β. These were obtained by placing a thermocouple on the inside surface of a specimen of boom similar to the pendulum material (fig. 11). A lamp was placed 4 in. from the boom center line and the lamp was turned on. After the thermocouple output indicated that an equilibrium temperature had been reached in the specimen, the recorder was turned on and a screen was quickly placed between the lamp and the specimen. From the resultant thermocouple output record, the value of B and β were obtained by

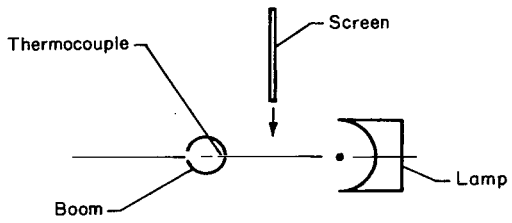

Figure 11.- Test arrangement for determination of B and β - lamp at $\Psi = 0$.

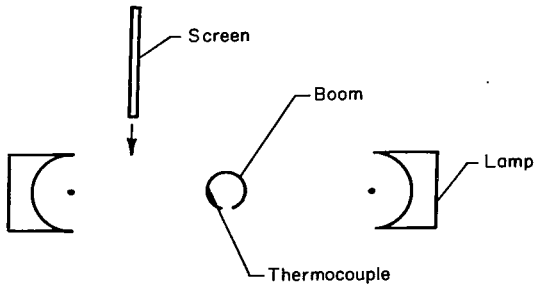

Figure 12.- Test arrangement for determination of B and β - two lamps at $\Psi = \pm 90°$.

a best fit to the solution of equation (13) for a step function $R(x,\phi,t)$. The same test was repeated with two lamps (fig. 12) to obtain data for the $\Psi = 90°$ case.

Comparison of Theory and Experiment

The values of B, β, and ζ (as determined from the free oscillation decay) can be substituted into the analytical model, and from the roots of the characteristic equation, the logarithmic decrement of the response can be determined. The comparison of the theoretical and experimental values of logarithmic decrement is shown in figure 13.

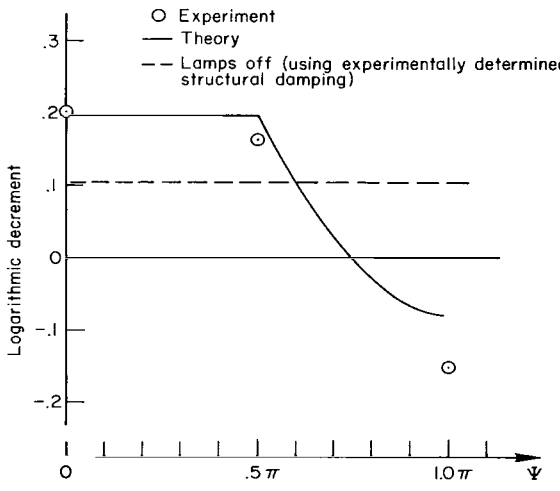

Figure 13.- Comparison of theoretical and experimental values of logarithmic decrement. Calculations based on 30° amplitude oscillation (fig. 10).

The theoretical curve of figure 13 is based on the structural damping (logarithmic decrement) values obtained from the experiments at amplitudes, Θ, of about 30° (fig. 10).[5] Correspondingly, the experimental data points are taken from figure 10 for the same amplitude. Since the data points of figure 10 are relatively parallel for different lamp positions, the choice of some other amplitude for the comparison in figure 13 would result in a shift of the ordinate of both theory and experiment. However, their relative location would remain unchanged.

[5]Although the theory is valid only for small angular displacements of the boom (θ), it should be noted that Θ represents the maximum angular displacement, therefore, good agreement should be expected for relatively large values of Θ.

CONCLUSIONS

1. Thermoelastic instability (thermal flutter) can occur and can be demonstrated in laboratory experiments.

2. Thermoelastic coupling can lead to a more stable system (add positive damping).

3. One-degree-of-freedom thermal flutter is possible and can be demonstrated readily with a torsional pendulum.

4. A small amplitude linear analysis has been presented that predicts the experimentally measured thermoelastic coupling for the torsional pendulum.

Ames Research Center
National Aeronautics and Space Administration
Moffett Field, Calif., 94035, March 27, 1969
124-08-06-02-00-21

REFERENCES

1. Augusti, G.: Instability of Struts Subject to Radiant Heat. Presented at the 12th International Congress of Applied Mechanics, Stanford, August 26-31, 1968. Meccanica, no. 3, 1968.

2. Yu, Y.: Thermally Induced Vibration and Flutter of a Flexible Boom. AIAA paper 69-21, Jan. 1969.

3. Koval, L. R.; Mueller, M. R.; and Paroczai, A. J.: Solar Flutter of a Thin-Walled Open-Section Boom. Presented at the Symposium on Gravity Gradient Attitude Stabilization, Aerospace Corp., El Segundo, Dec. 3-5, 1968.

4. Donohue, J. H.; and Frisch, H. P.: Thermoelastic Instability of Open Section Booms. Presented at the Symposium on Gravity Gradient Attitude Stabilization, Aerospace Corp., El Segundo, Dec. 3-5, 1968.

5. Timoshenko, S. P.: Theory of Bending, Torsion, and Buckling of Thin Walled Members of Open Cross Section. J. Franklin Institute, vol. 239, no. 4, April 1945, pp. 249-268.

6. Rimrott, Fred P. J.; and Elliott, Trevor: Torsion of Slit, Overlapped, Thin-Walled Tubes. J. Spacecraft Rockets, vol. 3, no. 6, June 1966, pp. 873-876.

7. Eckert, E. R. G.; and Drake, Robert M., Jr.: Heat and Mass Transfer. Second ed., McGraw-Hill, N. Y., 1959.

8. D'Azzo, John J.; and Houpis, Constantine H.: Feedback Control System Analysis and Synthesis. McGraw-Hill, N. Y., 1960.

"The aeronautical and space activities of the United States shall be conducted so as to contribute . . . to the expansion of human knowledge of phenomena in the atmosphere and space. The Administration shall provide for the widest practicable and appropriate dissemination of information concerning its activities and the results thereof."

—NATIONAL AERONAUTICS AND SPACE ACT OF 1958

NASA SCIENTIFIC AND TECHNICAL PUBLICATIONS

TECHNICAL REPORTS: Scientific and technical information considered important, complete, and a lasting contribution to existing knowledge.

TECHNICAL NOTES: Information less broad in scope but nevertheless of importance as a contribution to existing knowledge.

TECHNICAL MEMORANDUMS: Information receiving limited distribution because of preliminary data, security classification, or other reasons.

CONTRACTOR REPORTS: Scientific and technical information generated under a NASA contract or grant and considered an important contribution to existing knowledge.

TECHNICAL TRANSLATIONS: Information published in a foreign language considered to merit NASA distribution in English.

SPECIAL PUBLICATIONS: Information derived from or of value to NASA activities. Publications include conference proceedings, monographs, data compilations, handbooks, sourcebooks, and special bibliographies.

TECHNOLOGY UTILIZATION PUBLICATIONS: Information on technology used by NASA that may be of particular interest in commercial and other non-aerospace applications. Publications include Tech Briefs, Technology Utilization Reports and Notes, and Technology Surveys.

Details on the availability of these publications may be obtained from:

SCIENTIFIC AND TECHNICAL INFORMATION DIVISION

NATIONAL AERONAUTICS AND SPACE ADMINISTRATION

Washington, D.C. 20546